As previously stated, NN Ser belongs to the class of pre-cataclysmic binaries. These systems are thought to be born after the common-envelope evolution of originally wide pairs of unequal mass with orbital periods in the order of a few days. In the pre-cataclysmic state, the binaries exhibit shorter periods, consist then of a hot subdwarf or white dwarf primary and a main-sequence secondary and are surrounded by a planetary nebula which may later disperse. The secondary is believed to remain basically unaffected by this binary evolution process. Presently, we have at least some information on about 50 candidates, about one dozen being still associated with planetary nebulae. Only nine of these 50 systems show eclipses and provide sufficient spectral information to allow the determination of fairly reliable values of masses and radii of the components. Five systems are hot subdwarf/main-sequence binaries, the remaining four (including NN Ser) harbour white dwarf/K-M components. A thorough study of NN Ser will, therefore, also contribute to our knowledge of this interesting evolutionary state of binaries.

References

Appenzeller, I. et al.: 1998, *The Messenger* No. **94**, 1.
Catalán, M.S., Davey, S.C., Sarna, M.J., Smith, R.C., Wood, J.H.: 1994, *Mon.Not. R.Astron.Soc.* **269**, 879.
Häfner, R.: 1989a, *Astron.Astrophys.* **213**, L15.
Häfner, R.: 1989b, *The Messenger* No. **55**, 61.
Wood, J.H., Marsh, T.R.: 1991, *Astrophys. J.* **381**, 551.

E-mail: haefner@usm.uni-muenchen.de

The FORS Deep Field

I. APPENZELLER[1, 5], R. BENDER[3], A. BÖHM[2], N. DRORY[3], K. FRICKE[2], R. HÄFNER[3], J. HEIDT[1], U. HOPP[3], K. JÄGER[2], M. KÜMMEL[5], D. MEHLERT[1], C. MÖLLENHOFF[1], A. MOORWOOD[4], H. NICKLAS[2], S. NOLL[1], R. SAGLIA[3], W. SEIFERT[1], S. SEITZ[3], O. STAHL[1], E. SUTORIUS[1], T. SZEIFERT[4], S. WAGNER[1], B. ZIEGLER[2]

[1]Landessternwarte Heidelberg, [2]Universitäts-Sternwarte Göttingen, [3]Universitäts-Sternwarte München, [4]ESO Garching, [5]MPIA Heidelberg

1. Deep Fields

Watching the sky with the naked eye we can detect several thousand galactic stars but never more than two or three objects beyond our Milky Way galaxy. On the other hand, already images taken with small telescopes and photographic plates record in fields well outside the galactic plane more distant galaxies than galactic stars. Obviously, an increased sensitivity does not only allow us to see more objects, but, more importantly, we can look deeper into space. During the period when photographic plates were still the prime optical detectors, deep observations were usually carried out using Schmidt telescopes which allowed us to combine a deep look with a large field of view. Telescopes with larger apertures did not provide a great advantage since (because of the non-linearity and poor reproducibility of the photographic process) the flux (or magnitude) limit of photographic imaging was determined by the sky background, which could not be subtracted accurately. Only with the introduction of the essentially linear CCD detectors it became possible to observe objects with a surface brightness well below that of the sky. However, for manufacturing reasons, the achievable dimensions of CCDs are much smaller than those of large photographic plates. Therefore, imaging surveys reaching very faint magnitudes have, so far, been restricted to relatively small *Deep Fields*. Nevertheless, such deep-field surveys have proven to be exceedingly valuable in producing complete inventories of faint objects, for finding very distant objects, and for studying the properties and statistics of galaxies as a function of the evolutionary age of the universe.

Although the mean sky background can be determined and subtracted reliably from CCD frames, the photon noise of the sky, being of stochastic nature, cannot be eliminated. Therefore, even with CCDs, the achievable accuracy of faint-object photometry still depends on the amount of sky flux underlying the object images. Therefore, observations from space provide particularly favourable conditions for deep imaging and photometry since at most visual wavelengths the sky background is lower and since the absence of atmospheric seeing effects normally results in sharper images. It is not surprising, therefore, that two HST-based deep-field surveys (HDF and HDF-S) had a particularly strong scientific impact, providing a wealth of information and inspiring many follow-up studies.

2. Motivation for a FORS Deep Field

In spite of their great importance and success, the Hubble Deep Fields have some drawbacks. One obvious disadvantage is the, compared to modern ground-based faint-object cameras, relatively small field of view of the HST WFPC which limited the Hubble Deep
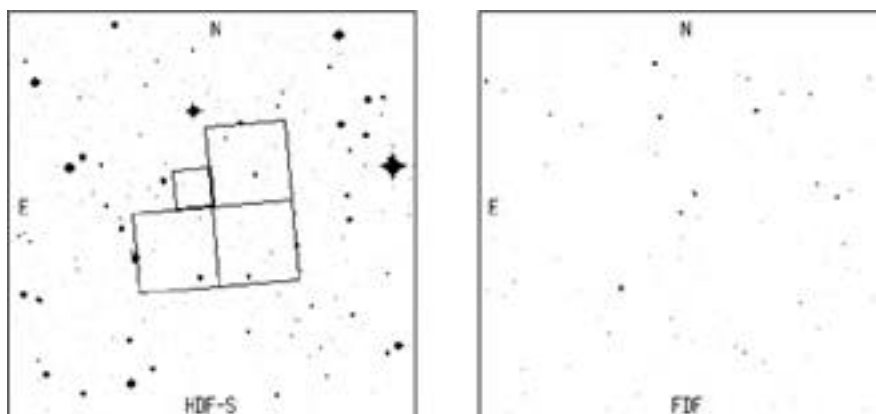

Figure 1: Digital Sky Survey plots of the FDF and of a field of the same size surrounding the HDF-S. Note the lower surface density of bright foreground objects and the absence of bright stars in the FDFregion.

Figure 2: True colour image of the inner 6′ × 6′ of the FORS Deep Field. North is up, East to the left.

Fields to areas of only about 6 square arcminutes. Moreover, the compared to present large ground-based telescopes relatively modest aperture of the HST requires very long integration times to collect a sufficient number of photons from faint objects. Finally, under optimal atmospheric conditions today's large ground-based telescopes with high quality cameras at good sites can reach practically the same image quality as the HST. This has been demonstrated during the past months with the combination of the ESO VLT and the HR mode of the FORS focal plane instruments where the best stellar images obtained so far showed FWHM values below the 2×0.1 arcsec pixel sampling resolution limit of the CCD. Since the HST WFPC has the same pixel size (which again undersamples the instru-

mental PSF), the images obtained with the FORS HR mode during the best seeing experienced so far at Paranal just match the resolution of single HST WFPC frames. Hence, by selecting observing periods of optimal seeing, at least at wavelength bands where the sky background is produced mainly outside the earth's atmosphere, modern ground-based telescopes with high-quality focal-plane instruments can in principle observe as deep as, or deeper than, the HST.

Unfortunately, a quick look at the Paranal seeing statistics shows that periods of seeing below 0.2 arcsec are so rare that observing programmes requiring such good seeing for sizeable amounts of time would require years to complete, even if all the time with excellent seeing would be allocated to

one such a programme. On the other hand, moderately good seeing occurs relatively often. According to ESO's VLT Site Selection WG report, seeing below 0.6 arcsec is to be expected for about 40 % of the time. At 0.6 arcsec the well-sampled VLT PSF is about 3 times larger and its surface about 10 times larger than for the HST WFPC, resulting for unresolved objects in a 10 times larger sky background. In wavelength bands with no significant atmospheric sky contribution, this results in an increase of the noise level by about a factor 3 and in a correspondingly lower signal-to-noise ratio. On the other hand, the VLT has an about 10 times larger collecting area, resulting in an increase of S/N by a factor 3. Therefore, for point sources at 0.6 arcsec seeing (and with no significant atmospheric contribution to the
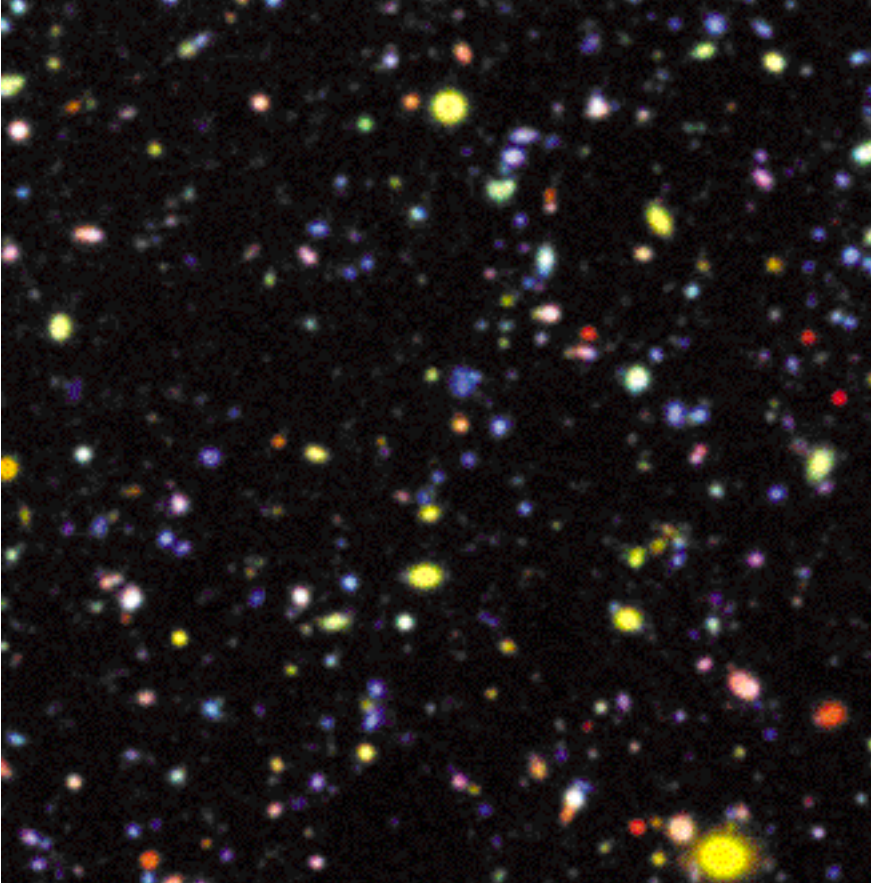
Figure 3: Enlargement of a 100″ × 100″ area of Figure 2.

sky background), the larger collecting area of the VLT just compensates the seeing effect on the photometric S/N. Hence for equal exposure times we get the same S/N as with the HST. For extended sources we in fact gain with the VLT. In the red spectral range, where we have strong atmospheric contributions to the sky background, the HST has a larger advantage compared to the VLT. At these wavelengths, the VLT is competitive only at better seeing conditions or with an increased total exposure time. Nevertheless, if periods of good seeing are selected and if a sufficient amount of observing time is invested, the VLT can look as deep as the HST. But with the larger FOV of the FORS instruments significantly larger statistical samples can be obtained in a single FORS field.

The above estimates show that FORS and the VLT provide an attractive alternative to HST for deep-field studies. But the estimates also show that in order to reach similar limiting magnitudes, comparable amounts of observing time have to be invested. Such large projects cannot be carried out easily as normal General Observer programmes at the VLT. For this reason, the consortium of German astronomical institutes (comprising the Heidelberg State Observatory (LSW) and the University Observatories of Göttingen and München) which – in co-operation with ESO – built the FORS instruments, decided to devote a significant fraction

of the guaranteed observing time, which the three institutes received for their effort, to observe a FORS Deep Field (FDF).

3. Field Selection and Observing Programme

Although under optimal seeing conditions the FORS instruments are most sensitive using the HR imaging mode, all FDF observations were carried out in the Standard Resolution (SR) mode. There were two reasons for using this mode: Firstly, the HR mode becomes superior only during periods of seeing below 0.4 arcsec, which at the VLT occurs only during less than 4 per cent of the time. Secondly, with the SR mode, having a FOV covering about 46 square arcmin (about 8 times that of the HST WFPC), we can potentially observe more objects and, by covering a larger volume of space, we may be less affected by local density variations and peculiarities.

A major disadvantage of the larger aperture of the VLT is that even moderately bright objects will produce CCD saturation effects already during relatively short exposure times. Moreover, because of the larger field, the chances of finding a bright star in the FORS FOV are greater than for the WFC. In order to keep the ratio between exposure times and readout periods of the individual frames at an acceptable value, deep photometry can be carried out with FORS economically only in fields which are free of stars brighter than about 19 mag. Therefore, apart from the usual criteria of the absence of significant galactic extinction, the absence of IR emission, and the absence of foreground galaxy clusters, the main criterion for the FDF was the absence of stars brighter than 19 mag. For this reason, it was not possible to use the surroundings of the southern Hubble Deep Field (HDF-S) for the FDF programme. As shown in Figure 1, there are too many bright foreground stars in and near the HDF-S to allow deep VLT exposures of this region. An additional criterion for the selection of the FDF was the presence of a distant (z > 3) QSO, which
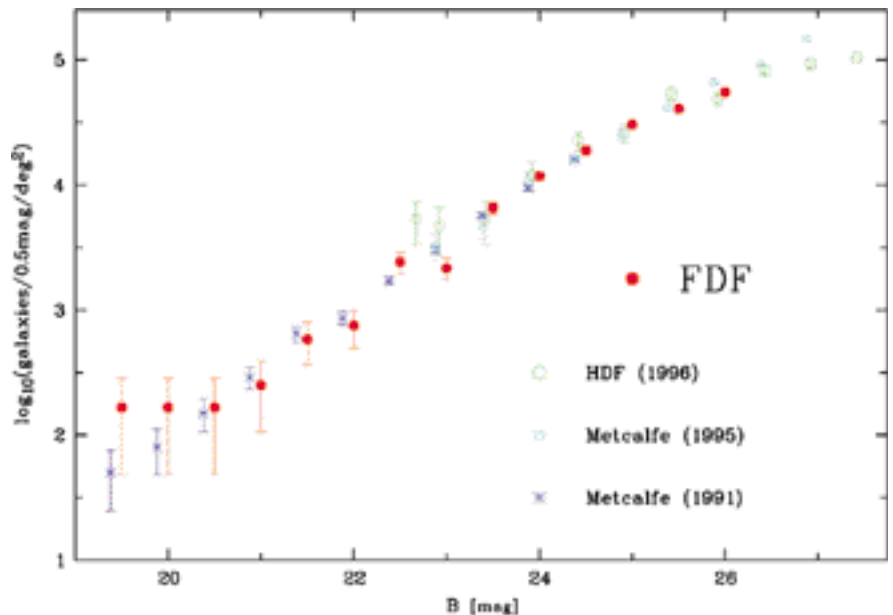

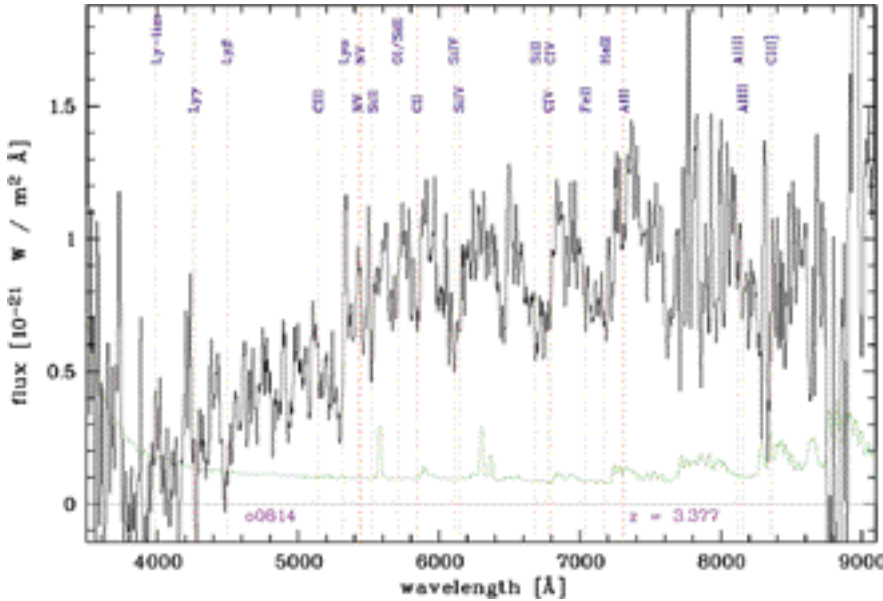Figure 4: Comparison of preliminary (bright) galaxy counts in the FDF with results from oth - er deep surveys.

Figure 5: Spectrum of a distant (z = 3.377) galaxy found in the FDF. The green line indicates the noise level, which varies with wavelength due to the night sky spectrum and the wave-length-dependent instrumental efficiency.

would allow us to study the intergalactic gas distribution along the line of sight. Finally, the field had to be observable well from Paranal. An analysis of various digital sky maps resulted in four fields matching these criteria. Test observations then showed that only one of the four field candidates was fully suited for our purpose. A true-colour image of this field (located at $\alpha_{2000} = 01^h06^m03.6^s$, $\delta_{2000} = -25° 45 46$) containing about 10^4 galaxies is reproduced in Figure 2. Figure 3 shows an enlarged subimage of a 100×100 area in the SE quadrant of Figure 2. The conspicuous blue galaxies have in most cases significant redshifts and are intrinsically UV-emitting galaxies with enhanced star formation at earlier cosmic epochs.

4. First Results

During the second half of 1999, we carried out a programme to obtain deep photometry in the U, B, g, R, and I bands (as well as in some selected narrow bands) of the FDF. In each of these filter bands we constructed deep images based on several hours of exposures obtained during good seeing conditions. Using an automatic extraction programme, we are presently generating a catalogue of the observed galaxies and their colours in the FDF. As soon as the catalogue is complete and in its final form, these data will be made public. We also started a statistical analysis of the detected objects and a photometric classification and photometric redshift derivation of all galaxies in the field. Since for the reliable classification of certain galaxy types NIR colours are of crucial importance, we also obtained in the fall of 1999 J- and

K-band frames of the FDF using SOFI at the NTT at ESO La Silla.

Figure 4 shows preliminary galaxy number counts (based on a small subset of the data) in the B band. As shown by the figure, at brighter magnitudes, the observed distribution fits well the galaxy surface density derived by other authors, indicating that the FDF is well suited as a study region. Although the observations revealed the presence of a moderately distant galaxy cluster in the SW corner of the field, this cluster is not rich enough to disturb the number counts significantly. With our final data, we hope to extend the comparison to the whole magnitude range observed with the HST.

For subsamples of objects found to be of particular interest from the photometric data, we began obtaining FORS low-resolution spectra. The main objective of this spectroscopic programme will be to study the dependence of the physical properties of galaxies on the cosmic age. According to present plans, most of the spectroscopy will be carried out during two GTO runs in fall 2000. A few MOS spectroscopic frames were already obtained in periods of poor seeing or non-photometric conditions during the 1999 photometric runs. Among the more than one hundred spectra thus obtained so far, we found already some interesting high-redshift galaxies and QSOs. In Figures 5 and 6, we present two examples of high-redshift galaxy spectra showing strong Lyman and high ionisation metallic lines and a strong UV continuum (indicating intense starburst activity) but no or only weak emission lines.

As already noted, the FDF was selected to include a known high redshift (z = 3.36) QSO. Figure 7 presents a blue FORS spectrum of this object. The figure clearly shows the presence of a rich forest of intergalactic lines of various types. A detailed study of these lines requires a higher spectral resolution than is feasible with FORS. Therefore, we applied for time with UVES at the VLT to obtain high-resolution spectra of this QSO. The resulting spectra will allow us to derive redshifts for the Lyα absorbers, which will be compared to the redshifts of the galaxies along the line of sight. In this way, we hope to identify some of the absorbers and to compare the distribution of galaxies and the absorbing gas clouds in the direction of the FDF. Finally, we note that we also
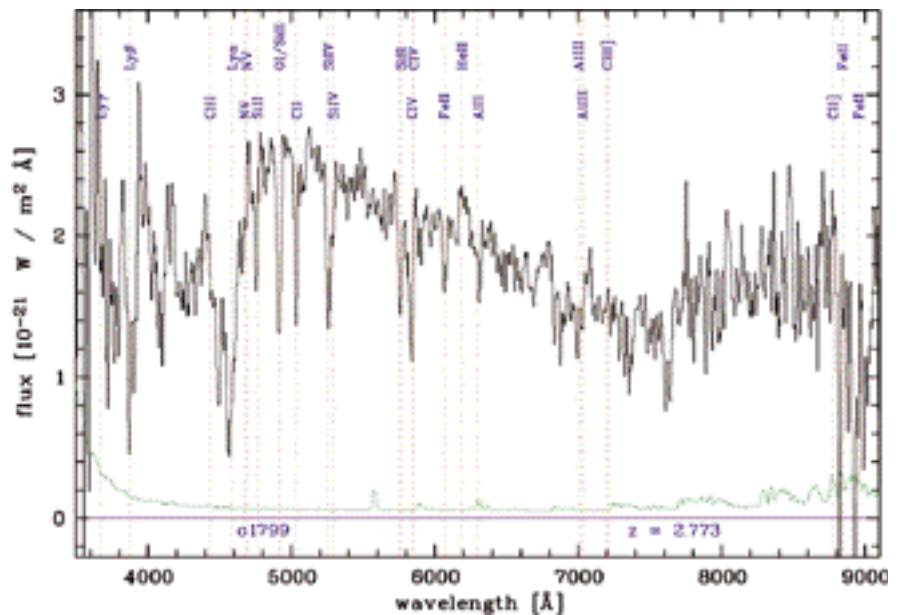

Figure 6. The spectrum of a z = 2.773 FDF galaxy. Note the strong (rest frame) UV continuum and absence of strong line emission.

initiated FDF follow-up investigations in other wavelength ranges. The most extensive of these follow-up studies is a mapping of the FDF at radio wavelengths which is being carried out in co-operation with colleagues from the MPI for Radioastronomy, Bonn, at the VLA.

At present our FDF project is still work in progress. While our deep photometric study can probably be completed within the next few months, the spectroscopic programme and the follow-up investigations may keep us (and other interested groups) busy for years to come. We hope – and are optimistic – that these studies will eventually result in new and important insights into the evolution of our universe, which will perhaps be reported in future issues of *The Messenger*.
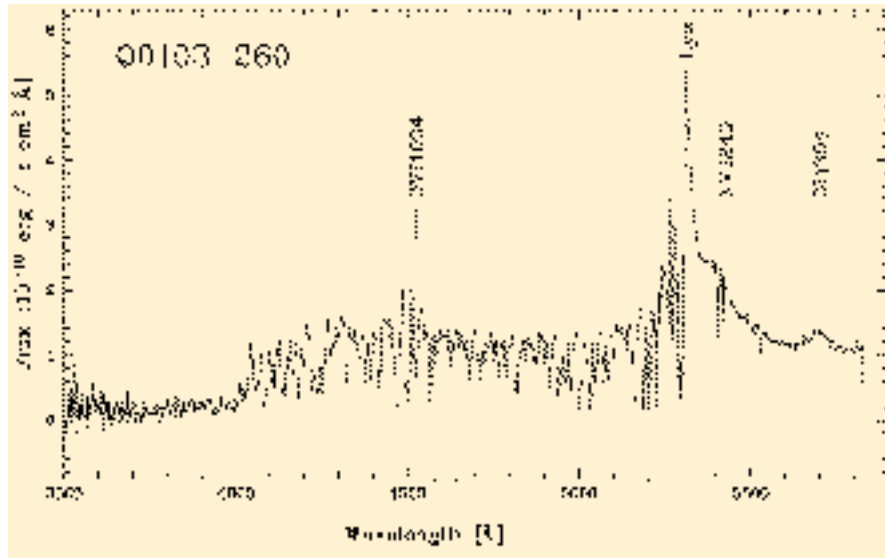

Figure 7: FORS spectrum of the Lyman forest of the FDF quasar Q0103-260.

Astronomical Image Resampling

N. DEVILLARD, ESO

1. Introduction

Resampling an image is a standard operation used in astronomical imaging for various tasks: changing the scale of an image to superimpose it on another, shifting an image by a non-integer offset, rotating an image by an arbitrary angle, or deforming an image to counter detector or optical deformations, are the usual operations in need of image resampling. In a more general way, this operation is referred to as *image warping* in the digital image processing world.

2. Sampling a Signal

The stellar light landing on an astronomical detector is a continuous optical signal. It is sampled by the detector at precise positions, yielding a regular grid of intensity values also known as pixels (for *picture elements,* often abbreviated to *pel).* The initial signal carries by definition an infinite amount of information (because of its continuity), but it has been reduced to a finite number of values by the detector system. The sampling theory has proved that it is possible to reconstruct the initial signal from

the knowledge of its samples only, provided that a certain number of assumptions are fulfilled.

In our case, we will assume that this is always the case, i.e. that the pixel sampling frequency is always greater than twice the greatest spatial frequency of the image (Shannon or Nyquist sampling). This is true for most ground-based telescopes because the instruments have been designed so, but this does not apply to some HST instruments for example. In that case, it is still possible to retrieve the signal, modulo some assumptions. This is not discussed in this paper.

3. Sampling Theory

This section provides some background about the sampling theory in general. For convenience, a simple 1-dimensional signal S(t) will be used as a conventional signal, because in this case the same rules apply to images understood as 2-dimensional signals (an intensity as a function of the pixel position on the detector).

The Fourier transform is a very convenient tool to perform an academic study of this case. It also helps to see the signal in another space to understand exactly what is happening during the various operations performed on it.

The representation of a signal $S(t)$ in Fourier space is a distribution that has no energy outside of a certain frequency range, i.e. it has non-zero values
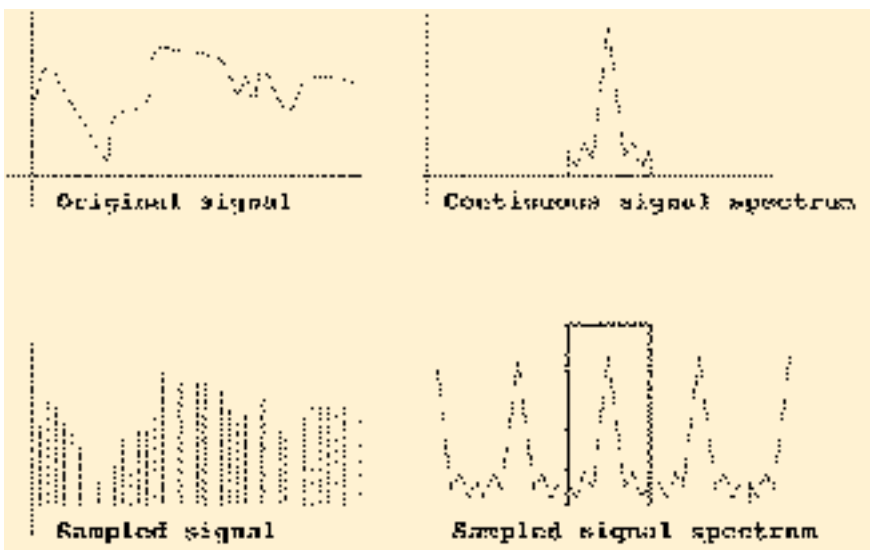

Figure 1: Top left is the original signal, top right its Fourier transform. Bottom left is the sampled signal and bottom right the Fourier transform of the sampled signal.